Modeling the electronic state of the high-T_c superconductor LaCuO: Phonon dynamics and charge response

Claus Falter,* Thomas Bauer, and Frank Schnetgöke
Institut für Festkörpertheorie, Westfälische Wilhelms-Universität, Wilhelm-Klemm-Strasse 10, 48149 Münster, Germany
(Received 28 December 2005; revised manuscript received 25 April 2006; published 5 June 2006)

A modeling of the normal state of the *p*-doped high-temperature superconductors (HTSC's) is presented. This is achieved starting from a more conventional metallic phase for optimal and overdoping and passing via the underdoped to the insulating state by consecutive orbital selective compressibility-incompressibility transitions in terms of sum rules for the charge response. The modeling is substantiated by corresponding phonon calculations. Extending investigations of the full dispersion and in particular of the strongly doping dependent anomalous phonon modes in LaCuO, which so far underpin our treatment of the density response of the electrons in the *p*-doped HTSC's, gives additional support for the modeling of the electronic state, compares well with recent experimental data and predicts the dispersion for the overdoped regime. Moreover, phonon densities of states have been calculated and compared for the insulating, underdoped, optimally doped, and overdoped state of LaCuO. From our modeling of the normal state a consistent picture of the superconducting phase also can be extracted qualitatively pointing in the underdoped regime to a phase ordering transition. On the other hand, the modeling of the optimal and overdoped state is consistent with a quasiparticle picture with a well defined Fermi surface. Thus, in the latter case a Fermi surface instability with an evolution of pairs of well defined quasiparticles is possible and can lead to a BCS-type ordering. So, it is tempting to speculate that optimal T_C in the HTSC's marks a crossover region between these two forms of ordering.

DOI: 10.1103/PhysRevB.73.224502 PACS number(s): 74.72.Dn, 74.25.Kc, 71.38.−k, 63.20.Dj

I. INTRODUCTION

In our microscopic theoretical description of the charge response, electron-phonon interaction (EPI) and lattice dynamics of the high-temperature superconductors (HTSC's) in the framework of the linear response approach we focus on the specific features of their solid-state chemistry. This is different from the overwhelming number of attempts relying on simplified models with strongly reduced model Hamiltonians. Nevertheless, this seems necessary since the phenomena observed in the cuprates hardly even occur in the other known compounds. One important feature neglected for example in the popular models of Hubbard type is the proximity of the HTSC's, even in the optimally doped case, to the layered ionic crystals where besides short-ranged correlations strong long-range Coulomb interaction and strong (nonlocal) EPI exists. In the absence of full *ab initio* methods for the HTSC's to tell us what the correct starting point would be, such insight is essential, in addition to the proximity of the materials to an antiferromagnetic state. Models with strongly reduced electronic degrees of freedom may be useful for the discussion of theoretical ideas in general rather than for detailed calculations of the material specifica of the cuprates.

The strong ionic nature of the HTSC's is modeled in our approach by an *ab initio* rigid ion model (RIM), used as a reference frame for the local ionic, rigid charge response and the EPI, respectively. The important and characteristic nonlocal, nonrigid contribution to the electronic density response and the EPI in the HTSC's is calculated in terms of microscopically well defined charge fluctuations (CF's) and dipole fluctuations (DF's). The latter are excitable on the electronic shells of the ions in the crystal. This is because most of the charge in the HTSC's contributing to bonding is concentrated on the latter. Additionally, covalent metallic features of bonding are approximatively taken into account.[1,2] In the calculations a sufficiently broad orbital freedom (Cu3*d*, Cu4*s*, and O2*p*), the full three-dimensional Coulomb interaction as well as the short-ranged local repulsions, in particular the important on-site repulsion mediated by the localized Cu3*d* orbitals, is considered quantitatively. All the resulting couplings appearing in the dynamical matrix and the EPI are microscopically well defined and can be calculated. The results obtained so far agree well with the experimental phonon dispersion. For a recent review, see Ref. 1.

The model for the electronic polarizability matrix[1,3] $\Pi_{\kappa\kappa'}(\mathbf{q})$ of the optimally and overdoped metallic state of the HTSC's, describing the kinetic part of the charge response, is obtained in a first step from the Kohn-Sham parameters (usually interpreted as bandstructure) within the local density approximation (LDA) of density functional theory (DFT). The indices κ, κ' denote the orbital degrees of freedom in the elementary cell of the crystal, i.e., Cu3*d*, Cu4*s*, and O2*p*. $\mathbf{q}$ is a wave vector in the first Brillouin zone. However, such a model, applied to LaCuO overestimates the coupling along the *c* axis and thus underestimates the real anisotropy in the cuprates. Modifications to improve the charge response along the ionic *c* axis have been investigated in Refs. 3 and 4. Given the nearly two-dimensional electronic structure of the cuprates and thus a very weak interlayer coupling, electron dynamics, and phonon dynamics will be on the same time scale in a small region around the *c* axis. This needs a nonadiabatic treatment with dynamical screening of the bare Coulomb interaction and phonon-plasmon mixing in the metallic state of the HTSC's.[1,4]

In the absence of a rigorous quantitative description for the insulating (undoped) state of the HTSC's, the model for $\Pi_{\kappa\kappa'}$ has been designed to be consistent with the character-

istic electronic charge response for an insulator with a gap in the charge excitation spectrum. This is achieved by fulfilling rigorous sum rules for the density response in terms of the polarizability matrix in the long-wavelength limit.[2,5] These sum rules, see Sec. III, can be considered as orbital resolved closed forms to represent the change of the charge response in a metal-insulator transition in terms of the electronic polarizability or the compressibility of the electronic system, respectively, as a primary tool to characterize the ground state.

Finally, a suitable model is proposed for the underdoped state of the *p*-doped HTSC's, where a description of the low-energy excitations remains a theoretical challenge and where the question of how the metallic charge conduction emerges from the doped insulator is poorly understood. This model describes a novel metallic state with an insulatorlike, incompressible charge response related to the localized Cu3*d* orbitals at the Cu sublattice interspersed with a metallic, compressible charge response related to the more delocalized O2*p* orbitals at the oxygen sublattices of the CuO plane. In this way a partial ordering of the conducting carriers in the CuO plane is obtained. With regard to our modeling of the metallic state for the optimally and overdoped HTSC's such an ergodicity breaking delocalization-localization transition in the underdoped state in terms of the compressibility means a compartmentalization of configuration space. This means that some parts of configuration space cannot be approached or are hardly accessible to the particles. On the other hand, this should be accompanied by a reciprocal compartmentalization of momentum space, according to the uncertainty relationship $\Delta x \Delta k \sim 1$. Indeed, angle-resolved photoemission spectroscopy (ARPES) studies in underdoped cuprates,[6–8] reporting a "two component" electronic structure with a pseudogap around $(\pi,0)$ and only part of the Fermi surface surviving as an "arc" around the node, point to compartmentalization of momentum space too. The compartmentalization of momentum space counteracts the reduction of the electron scattering rate brought about by the Pauli principle in a Fermi liquid, at least partially. Thus, the scattering rate and the lifetime of the carriers will no longer follow the well known scaling with energy and temperature of a Fermi liquid. Consequently, the normal state should display non-Fermi-liquid properties in our model for the underdoped state of the cuprates, also seen in the experiment. In the corresponding superconducting state an increase of the kinetic energy as in BCS by the "smearing" of the Fermi surface would not be present because the latter is not developed. On the other hand, phase coherence in a phase ordering scenario would enhance the mobility of pairs and decrease the kinetic energy. Such a description of a delocalization-localization crossover of the electronic structure (e.g., due to doping) accompanied by a pseudogap phenomenon in terms of consecutive orbital-selective compressibility-incompressibility transitions in the presence strong nonlocal EPI may also be useful to model the charge correlations in other systems besides the cuprates characterized by a mixture of localized and delocalized orbitals.

The article is organized as follows. In Sec. II the theory and modeling is briefly reviewed to set the frame. Section III presents our calculated results of the phonon dispersion for the underdoped and overdoped state of LaCuO. Moreover, the phonon anomalies related to the high-frequency oxygen bond-stretching modes and the phonon density of states for the insulating, underdoped, optimally doped, and overdoped state of LaCuO are calculated. A discussion of the modeling of the electronic state in the cuprates consistent with the corresponding phonon calculations is provided. Finally, a summary will be presented in Sec. IV.

II. SKETCH OF THE THEORY AND MODELING

From a general point of view our treatment of the electronic density response and lattice dynamics in terms of DF's and CF's can be considered as a microscopic (semi–*ab initio*) implementation of the phenomenological dipole-shell model or the charge-fluctuation models, respectively. For a general formulation of phenomenological models for lattice dynamics that use localized electronic variables as adiabatic degrees of freedom, see, for example, Ref. 9. This formulation covers shell models, bond-charge models, and charge-fluctuation models. While in this approach the coupling coefficients are treated as empirical fitting parameters, the essential point in our microscopic scheme is that all the couplings can be calculated.

In the following a survey of the theory and modeling is presented. A detailed description can be found in Ref. 5 and in particular in Ref. 10 where the calculation of the coupling parameters is presented.

The local part of the electronic charge response and the EPI is approximated in the spirit of the quasi-ion approach[11] by an *ab initio* RIM taking into account covalent ion softening in terms of (static) effective ionic charges calculated from a tight-binding analysis (TBA). In addition, scaling of the short-ranged part of certain pair potentials between the ions is performed to simulate further covalence effects in the calculation in such a way that the energy-minimized structure is as close as possible to the experimental one.[12] Structure optimization and energy minimization is very important for a reliable calculation of the phonon dynamics through the dynamical matrix.

The RIM with the corrections just mentioned then serves as an unbiased reference system for the description of the HTSC's and can be considered as a first approximation for the insulating state of these compounds. Starting with such an unprejudiced rigid reference system nonrigid electronic polarization processes are introduced in form of more or less localized electronic CF's at the outer shells of the ions. Especially in the metallic state of the HTSC's the latter dominate the nonlocal contribution of the electronic density response and the EPI and are particularly important in the CuO planes. In addition, anisotropic DF's are admitted in our approach,[3,10] which prove to be specifically of interest for the ions in the ionic layers mediating the dielectric coupling and for the polar modes. Thus, the basic variable of our model is the ionic density which is given in the perturbed state by

$$\rho_\alpha(\mathbf{r}, Q_\lambda, \mathbf{p}_\alpha) = \rho_\alpha^0(r) + \sum_\lambda Q_\lambda \rho_\lambda^{\mathrm{CF}}(r) + \mathbf{p}_\alpha \cdot \hat{\mathbf{r}} \rho_\alpha^{\mathrm{D}}(r). \quad (1)$$

ρ_α^0 is the density of the unperturbed ion, as used in the RIM, localized at the sublattice α of the crystal and moving

rigidly with the latter under displacement. The Q_λ and $\rho_\lambda^{\mathrm{CF}}$ describe the amplitudes and the form-factors of the CF's and the last term in Eq. (1) represents the dipolar deformation of an ion α with amplitude (dipole moment) $\mathbf{p}_\alpha$ and a radial density distribution ρ_α^D. $\hat{\mathbf{r}}$ denotes the unit vector in the direction of $\mathbf{r}$. The $\rho_\lambda^{\mathrm{CF}}$ are approximated by a spherical average of the orbital densities of the ionic shells calculated in LDA taking self-interaction effects (SIC's) into account. The dipole density ρ_α^D is obtained from a modified Sternheimer method in the framework of LDA-SIC.[10] All SIC calculations are performed for the average spherical shell in the orbital-averaged form according to Perdew and Zunger.[13] For the correlation part of the energy per electron ε the parametrization given in Ref. 13 has been used.

The total energy of the crystal is obtained by assuming that the density can be approximated by a superposition of overlapping densities ρ_α. The ρ_α^0 in Eq. (1) are also calculated within LDA-SIC taking environment effects, via a Watson sphere potential and the calculated static effective charges of the ions into account. The Watson sphere method is only used for the oxygen ions and the depth of the Watson sphere potential is set as the Madelung potential at the corresponding site. Such an approximation holds well in the HTSC's.[12,14] As a general rule, partial covalence reduces the amplitude of the static effective charges in mixed ionic-covalent compounds such as the HTSC's, because the charge transfer from the cations to the anions is not complete as in the entirely ionic case. Finally, applying the pair-potential approximation we get for the total energy

$$E(R,\zeta) = \sum_{\mathbf{a},\alpha} E_\alpha^{\mathbf{a}}(\zeta) + \frac{1}{2} \sum_{(\mathbf{a},\alpha)\neq(\mathbf{b},\beta)} \Phi_{\alpha\beta}(\mathbf{R}_\beta^{\mathbf{b}} - \mathbf{R}_\alpha^{\mathbf{a}}, \zeta). \quad (2)$$

The energy E depends on both the configuration of the ions $\{R\}$ and the electronic (charge) degrees of freedom (EDF) $\{\zeta\}$ of the charge density, i.e., $\{Q_\lambda\}$ and $\{\mathbf{p}_\alpha\}$ in Eq. (1). $E_\alpha^{\mathbf{a}}$ are the energies of the single ions. $\mathbf{a}$, $\mathbf{b}$ denote the elementary cells and α, β the corresponding sublattices. The second term in Eq. (2) is the interaction energy of the system, expressed in terms of anisotropic pair interactions $\Phi_{\alpha\beta}$. Both $E_\alpha^{\mathbf{a}}$ and $\Phi_{\alpha\beta}$ in general depend upon ζ via ρ_α in Eq. (1).

The pair potentials in Eq. (2) can be separated into long-ranged Coulomb contributions and short-ranged terms as follows:

$$\Phi_{\alpha\beta}(\mathbf{R},\zeta) = \frac{\mathcal{Z}_\alpha \mathcal{Z}_\beta}{R} - (\mathcal{Z}_\alpha \mathbf{p}_\beta + \mathcal{Z}_\beta \mathbf{p}_\alpha)\frac{\mathbf{R}}{R^3} + \frac{\mathbf{p}_\alpha \cdot \mathbf{p}_\beta}{R^3} - 3\frac{(\mathbf{p}_\alpha \cdot \mathbf{R})(\mathbf{R} \cdot \mathbf{p}_\beta)}{R^5} + \tilde{\Phi}_{\alpha\beta}(\mathbf{R},\zeta), \quad (3)$$

$$\tilde{\Phi}_{\alpha\beta}(\mathbf{R},\zeta) = K_\alpha U_\beta(\mathbf{R},\zeta) + K_\beta U_\alpha(\mathbf{R},\zeta) + W_{\alpha\beta}(\mathbf{R},\zeta) + G_{\alpha\beta}(\mathbf{R},\zeta). \quad (4)$$

The first term in Eq. (3) describes the long-ranged ion-ion, the second the dipole-ion and the third and fourth term the dipole-dipole interaction. $\mathcal{Z}_\alpha$ and $\mathcal{Z}_\beta$ are the variable charges of the ions in case the CF's are excited. The latter reduce to the ionic charges for rigid ions. K_α and K_β are the charges of the ion cores. The remaining term in Eq. (3) given in Eq. (4) represents the short-ranged interactions. These short-ranged contributions to the pair potentials are expressed by the following integrals:

$$U_\alpha(\mathbf{R},\zeta) = -\int d^3r \rho_\alpha(\mathbf{r},\zeta)\left(\frac{1}{|\mathbf{r}-\mathbf{R}|} - \frac{1}{R} - \frac{\mathbf{r}\cdot\mathbf{R}}{R^3}\right), \quad (5)$$

$$W_{\alpha\beta}(\mathbf{R},\zeta) = \int d^3r \int d^3r' \left[\rho_\alpha(\mathbf{r},\zeta)\rho_\beta(\mathbf{r}',\zeta)\left(\frac{1}{|\mathbf{r}-\mathbf{r}'-\mathbf{R}|} - \frac{1}{R} - \frac{(\mathbf{r}+\mathbf{r}')\cdot\mathbf{R}}{R^3}\right)\right], \quad (6)$$

$$G_{\alpha\beta}(\mathbf{R},\zeta) = \int d^3r \{\rho_{\alpha\beta}(\mathbf{r},\zeta)\epsilon[\rho_{\alpha\beta}(\mathbf{r},\zeta)] - \rho_\alpha(\mathbf{r},\zeta)\epsilon[\rho_\alpha(\mathbf{r},\zeta)] - \rho_\beta(\mathbf{r}-\mathbf{R},\zeta)\epsilon[\rho_\beta(\mathbf{r}-\mathbf{R},\zeta)]\}, \quad (7)$$

with

$$\rho_{\alpha\beta}(\mathbf{r},\zeta) = \rho_\alpha(\mathbf{r},\zeta) + \rho_\beta(\mathbf{r}-\mathbf{R},\zeta). \quad (8)$$

$K_\alpha U_\beta(\mathbf{R},\zeta)$ yields the short-ranged contribution of the interaction between the core α and the density ρ_β according to Eq. (1). $W_{\alpha\beta}(\mathbf{R},\zeta)$ represents the short-ranged Coulomb contribution of the interaction of the density ρ_α with the density ρ_β. $G_{\alpha\beta}(\mathbf{R},\zeta)$ is the sum of the kinetic one-particle- and the exchange-correlation (XC) contribution of the interaction between the two ions.[10] The short-ranged part of the potentials and the various coupling coefficients are calculated numerically for a set of distances R between the ions. The corresponding results are than described by an analytical function of the form

$$f(R) = \pm \exp\left(\alpha + \beta R + \frac{\gamma}{R}\right). \quad (9)$$

α, β, and γ in Eq. (9) are fit parameters.

From the adiabatic condition

$$\frac{\partial E(R,\zeta)}{\partial \zeta} = 0 \quad (10)$$

an expression for the atomic force constants, and accordingly the dynamical matrix in harmonic approximation can be derived:

$$t_{ij}^{\alpha\beta}(\mathbf{q}) = [t_{ij}^{\alpha\beta}(\mathbf{q})]_{\mathrm{RIM}} - \frac{1}{\sqrt{M_\alpha M_\beta}} \sum_{\kappa,\kappa'} [B_i^{\kappa\alpha}(\mathbf{q})]^* [C^{-1}(\mathbf{q})]_{\kappa\kappa'} B_j^{\kappa'\beta}(\mathbf{q}). \quad (11)$$

The first term on the right hand side denotes the contribution from the RIM. M_α, M_β are the masses of the ions and $\mathbf{q}$ is a wave vector from the first Brillouin zone (BZ).

The quantities $\mathbf{B}(\mathbf{q})$ and $C(\mathbf{q})$ in Eq. (11) represent the Fourier transforms of the electronic coupling coefficients as calculated from the energy in Eq. (2), or the pair potentials in Eqs. (3)–(8), respectively:

$$\mathbf{B}_{\kappa\beta}^{\mathbf{ab}} = \frac{\partial^2 E(R,\zeta)}{\partial \zeta_\kappa^{\mathbf{a}} \partial R_\beta^{\mathbf{b}}}, \tag{12}$$

$$C_{\kappa\kappa'}^{\mathbf{ab}} = \frac{\partial^2 E(R,\zeta)}{\partial \zeta_\kappa^{\mathbf{a}} \partial \zeta_{\kappa'}^{\mathbf{b}}}. \tag{13}$$

κ denotes the EDF [CF and DF in the present model, see Eq. (1)] in an elementary cell. The $\mathbf{B}$ coefficients describe the coupling between the EDF and the displaced ions (bare electron-phonon coupling), and the coefficients C determine the interaction between the EDF. The phonon frequencies $\omega_\sigma(\mathbf{q})$ and the corresponding eigenvectors $\mathbf{e}^\alpha(\mathbf{q}\sigma)$ of the modes $(\mathbf{q}\sigma)$ are obtained from the secular equation for the dynamical matrix in Eq. (11), i.e.,

$$\sum_{\beta,j} t_{ij}^{\alpha\beta}(\mathbf{q}) e_j^\beta(\mathbf{q}) = \omega^2(\mathbf{q}) e_i^\alpha(\mathbf{q}). \tag{14}$$

Equations (11)–(14) are generally valid and, in particular, are independent of the specific model for the decomposition of the perturbed density in Eq. (1) and the pair approximation Eq. (2) for the energy. The lengthy details of the calculation of the coupling coefficients $\mathbf{B}$ and C cannot be reviewed in this paper. They are presented in Ref. 10. In this context we remark that the coupling matrix $C_{\kappa\kappa'}(\mathbf{q})$ of the EDF-EDF interaction, whose inverse appears in Eq. (11) for the dynamical matrix, can be written in matrix notation as

$$C = \Pi^{-1} + \tilde{V}. \tag{15}$$

Π^{-1} contains the kinetic part to the interaction C and $\tilde{V}$ the Hartree and exchange-correlation contribution. C^{-1} needed for the dynamical matrix and the EPI is closely related to the (linear) density response function (matrix) and to the inverse dielectric function (matrix) ε^{-1}, respectively.

Only very few attempts have been made to calculate the phonon dispersion and the EPI of the HTSC's using the linear response method in form of density functional perturbation theory (DFPT) within LDA.[15–17] These calculations correspond to calculating Π and $\tilde{V}$ in DFT-LDA and for the *metallic* state only. On the other hand, in our microscopic modeling DFT-LDA-SIC calculations are performed for the various densities in Eq. (1) in order to obtain the coupling coefficients $\mathbf{B}$ and $\tilde{V}$. Including SIC is particularly important for localized orbitals such as Cu3*d* in the HTSC's. SIC as a correction for a single particle term is not a correlation effect, which per definition cannot be described in a single particle theory, but SIC is important for contracting in particular the localized Cu3*d* orbitals. The latter are correlated orbitals and so we use sometimes in this paper the phrase "correlated" Cu3*d* states or orbitals, respectively. Our theoretical results for the phonon dispersion, which compare well with the experiments,[1,3] demonstrate that the approximative calculation of the coupling coefficients in our approach is sufficient, even for the localized Cu3*d* states, see also Sec. III. Written in matrix notation we get for the density response matrix the relation

$$C^{-1} = \Pi(1 + \tilde{V}\Pi)^{-1} \equiv \Pi\varepsilon^{-1}, \quad \varepsilon = 1 + \tilde{V}\Pi. \tag{16}$$

The CF-CF submatrix of the matrix Π can approximatively be calculated for the metallic (but not for the undoped and underdoped) state of the HTSC's from a TBA of a single particle electronic bandstructure. In this case the electronic polarizability Π in tight-binding representation reads

$$\Pi_{\kappa\kappa'}(\mathbf{q},\omega=0) = -\frac{2}{N}\sum_{n,n',\mathbf{k}} \frac{f_{n'}(\mathbf{k}+\mathbf{q}) - f_n(\mathbf{k})}{E_{n'}(\mathbf{k}+\mathbf{q}) - E_n(\mathbf{k})} \times [C_{\kappa n}^*(\mathbf{k}) C_{\kappa n'}(\mathbf{k}+\mathbf{q})] \times [C_{\kappa' n}^*(\mathbf{k}) C_{\kappa' n'}(\mathbf{k}+\mathbf{q})]^*. \tag{17}$$

f, E, and C in Eq. (17) are the occupation numbers, the single-particle energies and the expansion coefficients of the Bloch functions in terms of tight-binding functions.

The self-consistent change of an EDF on an ion induced by a phonon mode $(\mathbf{q}\sigma)$ with frequency $\omega_\sigma(\mathbf{q})$ and eigenvector $\mathbf{e}^\alpha(\mathbf{q}\sigma)$ can be derived in the form

$$\delta\zeta_\kappa^{\mathbf{a}}(\mathbf{q}\sigma) = \left[-\sum_\alpha \mathbf{X}^{\kappa\alpha}(\mathbf{q}) \mathbf{u}_\alpha(\mathbf{q}\sigma)\right] e^{i\mathbf{q}\cdot\mathbf{R}_\kappa^{\mathbf{a}}} \equiv \delta\zeta_\kappa(\mathbf{q}\sigma) e^{i\mathbf{q}\cdot\mathbf{R}^{\mathbf{a}}}, \tag{18}$$

with the displacement of the ions

$$\mathbf{u}_\alpha^{\mathbf{a}}(\mathbf{q}\sigma) = \left(\frac{\hbar}{2M_\alpha \omega_\sigma(\mathbf{q})}\right)^{1/2} \mathbf{e}^\alpha(\mathbf{q}\sigma) e^{i\mathbf{q}\cdot\mathbf{R}^{\mathbf{a}}} \equiv \mathbf{u}_\alpha(\mathbf{q}\sigma) e^{i\mathbf{q}\cdot\mathbf{R}^{\mathbf{a}}}. \tag{19}$$

The self-consistent response per unit displacement of the EDF in Eq. (18) is calculated in linear response theory as

$$\mathbf{X}(\mathbf{q}) = \Pi(\mathbf{q})\varepsilon^{-1}(\mathbf{q})\mathbf{B}(\mathbf{q}) = C^{-1}(\mathbf{q})\mathbf{B}(\mathbf{q}). \tag{20}$$

A measure of the strength of the EPI for a certain phonon mode $(\mathbf{q}\sigma)$ is provided by the change of the self-consistent potential in the crystal felt by an electron at same space point $\mathbf{r}$ in this mode, i.e., $\delta V_{\text{eff}}(\mathbf{r},\mathbf{q}\sigma)$. Averaging this quantity with the corresponding density form factor $\rho_\kappa(\mathbf{r}-\mathbf{R}_\kappa^{\mathbf{a}})$ at the EDF located at $\mathbf{R}_\kappa^{\mathbf{a}}$, we obtain

$$\delta V_\kappa^{\mathbf{a}}(\mathbf{q}\sigma) = \int dV \rho_\kappa(\mathbf{r}-\mathbf{R}_\kappa^{\mathbf{a}}) \delta V_{\text{eff}}(\mathbf{r},\mathbf{q}\sigma). \tag{21}$$

This gives a measure for the strength of the EPI in the mode $(\mathbf{q}\sigma)$ mediated by the EDF considered. For an expression of $\delta V_\kappa^{\mathbf{a}}(\mathbf{q}\sigma)$ in terms of the coupling coefficients in Eqs. (12) and (13), see Ref. 1. From our calculations for LaCuO large values for $\delta V_\kappa^{\mathbf{a}}(\mathbf{q}\sigma)$ are found, in particular for the phonon anomalies and even larger for the nonadiabatic *c*-axis phonons in the metallic phase, mixing with the plasmon.

The generalization for the quantity Π in Eqs. (15) and (16) needed for the kinetic part of the charge response in the nonadiabatic regime, where dynamical screening effects must be considered, can be achieved by adding $(\hbar\omega + i\eta)$ to the differences of the single-particle energies in the denominator of the expression for Π in Eq. (17). Other possible nonadiabatic contributions to C related to dynamical exchange-correlation effects and the phonons themselves are beyond the scope of the present model. The coupled-mode frequencies of the phonons and the plasmons must be deter-

mined self-consistently from the secular equation (11) for the dynamical matrix which now contains the frequency ω implicitly via Π in the response function C^{-1}. Analogously, the dependence on the frequency is transferred to the quantity $\mathbf{X}$ in Eq. (20) and thus to $\delta\zeta_\kappa$ and δV_κ in Eqs. (18) and (21), respectively. Such a nonadiabatic approach is necessary for a description of the interlayer phonons and the charge response within a small region around the c axis.[1,4]

III. RESULTS AND DISCUSSION

A. A modeling of the electronic charge response and corresponding phonon calculations

An important question remains as to how to discriminate between the charge response of the metallic and insulating state of the HTSC's. The latter cannot be obtained within the LDA and a realistic quantitative description to calculate the irreducible polarization part $\Pi_{\kappa\kappa'}(\mathbf{q})$ for the HTSC's is not available. However, a general criterion follows from the different analytic behavior of the polarizability in the long-wavelength limit $(\mathbf{q}\rightarrow\mathbf{0})$ in both phases.[1,5] In the metallic phase the electronic partial density of states (PDOS) at the Fermi level $Z_\kappa(\varepsilon_F)$ is related to the polarizability matrix for $(\mathbf{q}\rightarrow\mathbf{0})$ according to

$$\sum_{\kappa'}\Pi_{\kappa\kappa'}(\mathbf{q}\rightarrow\mathbf{0})=Z_\kappa(\varepsilon_F), \tag{22}$$

and the total density of states at energy ε is given by

$$Z(\varepsilon)=\sum_{\kappa}Z_\kappa(\varepsilon). \tag{23}$$

On the other hand, for the insulating state we obtain the sum rules

$$\sum_{\kappa'}\Pi_{\kappa\kappa'}(\mathbf{q}\rightarrow\mathbf{0})=\mathcal{O}(q) \tag{24}$$

and

$$\sum_{\kappa\kappa'}\Pi_{\kappa\kappa'}(\mathbf{q}\rightarrow\mathbf{0})=\mathcal{O}(q^2). \tag{25}$$

The sum $\Sigma_{\kappa\kappa'}\Pi_{\kappa\kappa'}(\mathbf{q}\rightarrow\mathbf{0})$ is equal to ρ^2K with ρ the average density and K the compressibility of the electronic system. The latter provides a measure of the gap in the electronic spectrum because K vanishes as a function of the chemical potential in the gap region. Equations (22)–(25), respectively, can be considered as an orbital resolved closed form to describe the metal-insulator transition in terms of the polarizability or the compressibility of the electronic system, respectively. This is a primary tool to characterize the corresponding ground state. Such orbital selective sum rules are particularly useful in the proximity to a Mott insulating phase where different from the band insulator the internal degrees of freedom, orbital (and spin), approximatively survive. In order to fulfil the sum rules above, in case of the insulating state, in contrast to the metallic state, off-diagonal elements of the polarizability matrix describing nonlocal polarization processes necessarily must occur and interfere in order to correlate the charge response in such a way that Eqs. (24) and (25) are satisfied.

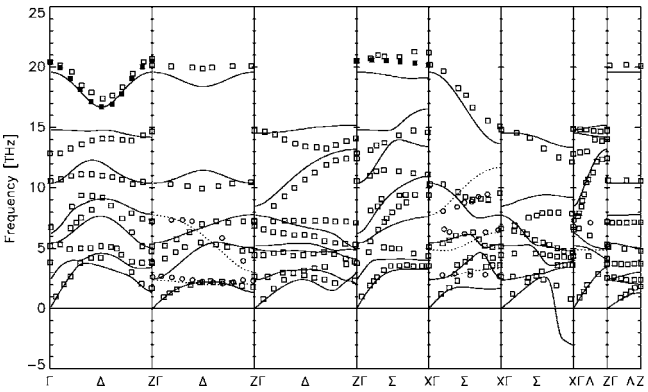

FIG. 1. Calculated phonon dispersion of LaCuO in the tetragonal structure in the main symmetry directions $\Delta\sim(1,0,0)$, $\Sigma\sim(1,1,0)$, and $\Lambda\sim(0,0,1)$ in the model for the optimally doped state. The various symbols representing the experimental results indicate different irreducible representations (ID's). Open symbols are for $La_{1.9}Sr_{0.1}CuO_4$ (Ref. 18) and solid symbols for $La_{1.85}Sr_{0.15}CuO_4$ (Ref. 19). The arrangement of the panels from left to right according to the different ID's is as follows: $|\ \Delta_1\ |\ \Delta_2(\cdots,\circ)$, $\Delta_4(—,\square)\ |\ \Delta_3\ |\ \Sigma_1\ |\ \Sigma_2(\cdots,\circ)$, $\Sigma_4(—,\square)\ |\ \Sigma_3\ |\ \Lambda_1(—,\square)$, $\Lambda_2(\cdots,\circ)\ |\ \Lambda_3\ |$

Physically this is related to the fact that in an insulator a perturbation, e.g., a change of the electron-ion potential, is only incompletely screened. Consequently, the selfconsistent change of the potential at the orbital degree of freedom κ' nonlocally contributes to the CF's of the orbital $\kappa\neq\kappa'$ in the unit cell. This is quite different from the metallic case where the diagonal elements of $\Pi_{\kappa\kappa'}$ dominate and off-diagonal elements can be neglected in most cases. As mentioned in the Introduction, the model for the polarizability of the metallic state is based on LDA calculations which, however, have to be modified to correct for the overestimation of the c-axis coupling in LDA-based investigations.[3] So, a model taking into account Cu3d, 4s, 4p, and $O_{xy}2p$ orbitals in the CuO plane results.[3] In contrast to the Cu4s orbital the effect of the Cu4p orbital on the phonon dynamics is only weak, so we have neglected the latter in the present calculations and enhanced the contribution of Π(Cu4s) slightly. In addition, the CF's also anisotropic DF's are taken into account.

The resulting calculated phonon dispersion is shown in Fig. 1. We get an overall agreement with the experimental dispersion curves. A few branches show larger deviations between experiment and theory. However, in particular the important phonon anomalies (high-frequency oxygen bond-stretching modes), which are a major theme in the recent literature and the present paper, too, are well described by our theory, see Fig. 4 below. This also holds true for the steep Λ_1 branch which results from the large anisotropy of the real material and cannot be described with pure LDA based calculations leading to an overestimation of the coupling along the c axis, see Ref. 3. Freezing-in the unstable Σ_3 tilt mode at the X point correctly indicates the experimentally observed structural phase transition from the high-temperature tetragonal (HTT) to the low-temperature orthorhombic (LTO)

structure. The actual transition, of course, cannot be studied in the harmonic approximation because the anharmonic contribution to the energy must be considered.[20] However, from our calculations in Ref. 1 we find that the soft tilt mode found in HTT is stabilized in LTO in harmonic approximation and thus the structural transition is essentially driven by the long-ranged ionic forces in the material.

A nonempirical potential-induced breathing (PIB) model[21] such as our model reflects the strong tendencies to ionic forces in the HTSC's. This model also correctly predicts, that the tetragonal structure is unstable to the *X*-point tilt mode. However, it cannot be applied to the metallic phase. Moreover, other unstable phonon branches are found in this model. The width of the phonon spectrum is considerably overestimated. For example, the PIB result for the planar oxygen breathing mode at the *X* point in the insulating phase is about 34 THz in comparison to the experiment ($\sim$21.8 THz) and to our calculated result of 21.6 THz, see Fig. 4. The PIB results are comparable to our calculations performed with the *ab initio* rigid ion model using nominal ionic charges,[5] neglecting the covalence correction for the ionic charges and the pair potential. Taking the latter effects into account, as mentioned in Sec. II, the correct width of the spectrum is obtained and, with the exception of the tilt mode at *X*, all unstable phonon branches disappear.[12] So, we obtain a suitable reference system for the HTSC which allows for the investigation of the additional nonlocal, nonrigid screening effects in terms of CF's and DF's.

Empirical shell model calculations for the lattice dynamics of several cuprates have been performed in Ref. 18. The fitting to the experimental results is quite satisfactorily emphasizing again the importance of the ionic forces. However, in the fitting the harmonic *X*-point tilt mode was assumed to be stable, which is at least questionable, because of the low-temperature orthorhombic structure. For a description of the metallic phase free-carrier screening of the homogeneous electron gas is additional assumed, but the softening of the phonon anomalies can not be accounted for by this type of screening. On the other hand, our calculations, see Fig. 1, lead to very good results for the phonon anomalies. Accordingly, we can relate the anomalous softening to the characteristic ionic, inhomogeneous electronic structure of the HTSC, leading to strong nonlocal EPI in terms of localized CF's in the outer shells of the ions controlled by the coupling coefficient C in Eq. (15).

In the model for the insulating phase in order to simulate stronger correlation effects as in the metal Cu4*s* orbitals are neglected and only the CF's of the Cu3*d* orbitals at the Cu and O2*p* orbitals at the O_{xy} are considered as on site CF's and the polarizability is adjusted so as to obey the sum rules from Eq. (24). The calculated results for the phonon dispersion can be found in Ref. 3. Similarly as for the metallic state a good agreement with the experiments is obtained. In particular, a significant reduction of the phonon anomalies as compared to the optimally doped material is well reproduced and attributed to the incompressibility of the electronic state. Including the screening contribution via anisotropic DF's, the longitudinal and transverse optical modes of A_{2u} and E_u symmetry are well described.

An *ab initio* calculation of the polarizability Π for the HTSC's, which in addition to strong electron correlations also should include the strong nonlocal EPI found in our calculations in the self-energy of the electrons, seems not possible in the near future. In particular this holds for the insulating and underdoped state. However, modeling Π according to the sum rules (22)–(25) guarantees that the constraints on the charge response in the different phases are fulfilled and, moreover, allows for the possibility to theoretically design condensed matter states with properties between that of a conventional metal and an insulator, respectively. This seems necessary to describe the physics in the underdoped cuprates where a strange metallic state does appear. Our modeling of the correlation phenomenon and the delocalization-localization transition from the metallic state of the HTSC's via the underdoped state to the undoped (insulating) state has been achieved with help of the sum rules by consecutive orbital selective compressibility-incompressibility transitions, see Ref. 2, and for a detailed review Ref. 1. Starting from the metallic side, representing in our model the doping range from optimally doped to overdoped, all the admitted orbitals, i.e., Cu3*d*, 4*s*, and O2*p*, are taken to be compressible, metallic consistent with an emerging quasiparticle description and a well defined Fermi surface. The corresponding sum rules appropriate for such a situation are given by Eqs. (22) and (23) with *all* the $Z_\kappa(\varepsilon_F)$ different from zero. Our calculation of the orbital occupation numbers[12] from a TBA of the first principles electronic (metallic) bandstructure of LaCuO (Ref. 22) indicates that in addition the Cu3*d* in particular the more delocalized Cu4*s* state must be included as an additional EDF at the Cu site. This, as already mentioned, is different from our modeling of the insulating and underdoped state where we have neglected a contribution from the Cu4*s* orbitals and only used the localized Cu3*d* and the O2*p* orbitals as EDF's in order to simulate stronger correlation effects in these states.

Approaching the delocalization-localization transition from the metallic region when *p* doping is decreased first the Cu3*d* component of the wave function is admitted in our model to become incompressible, insulatorlike in the underdoped regime by assuming that the corresponding single particle density of states $Z_\kappa(\varepsilon)$ is suppressed at the Fermi level for the correlated localized Cu3*d* orbitals, because of the cost in energy from hopping of the charge carrier to the Cu sites, but not so for the more delocalized O2*p* orbitals at the O_{xy} sublattices in the CuO plane where the holes are predominantly injected to in *p*-type cuprates. So, we have an orbital selective compressible, metallic charge response for the O2*p* orbitals with a renormalized PDOS $\tilde{Z}_\kappa(\varepsilon_F)$ and the holes tend to accumulate in the region of suppressed antiferromagnetism. Altogether, we have a loss in the density of states (pseudogap, correlation gap) at the Fermi level. Thus, the quasiparticle picture [$Z_\kappa(\varepsilon_F \neq 0)$ for *all* κ] consistent with our modeling of the metallic state for optimally to overdoping no longer holds in the underdoped state. The related compartmentalization of phase space can be expected to be the reason for the strange metallic behavior observed in the underdoped cuprates with an ill defined Fermi surface. The corresponding electronic state for this model [pseudogap model (PGM)] expressing the dichotomy between a localized

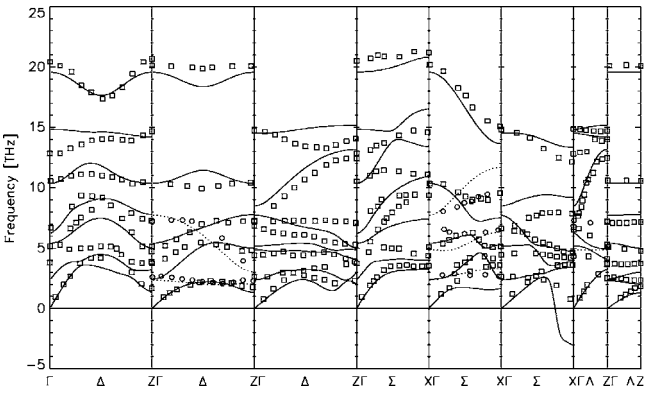

FIG. 2. Same as Fig. 1 with the calculated results from the model for the underdoped state.

and delocalized component has been defined by the following sum rule:[2]

$$\sum_{\kappa'} \Pi_{\kappa\kappa'}(\mathbf{q} \to \mathbf{0}) = \begin{cases} \mathcal{O}(q), & \text{Cu3}d, \\ \tilde{Z}_{\kappa}(\varepsilon_F), & \text{O2}p. \end{cases} \tag{26}$$

We realize from this equation, that nonlocal polarization processes are necessary to depress the density of states at ε_F via the Cu3d component and correspondingly the low energy single particle excitations. Finally, near half filling in addition to Cu3d, the O2p component of the electronic state has been modeled as incompressible too, and the charge-transfer insulator is formed according to the sum rules (24), (25) for both the Cu3d and O2p orbitals.

The phonon dispersion curves for our model of the underdoped state with an incompressible insulatorlike, charge response of the Cu3d orbital at the Cu sublattice and a compressible, metallic charge response of the O2p orbitals at the O_{xy} sublattice in the CuO plane is displayed in Fig. 2 and compared with experimental inelastic neutron results for underdoped LaCuO. The agreement of the calculations, which also include anisotropic DF's in addition to the CF's of Cu3d and O2p type, is good and of similar quality as the calculated results for optimally doped state in Fig. 1 and the insulating state in Ref. 3. Comparing the calculations in Figs. 1 and 2 essential differences are only found for the phonon anomalies (highest Δ_1 and Σ_1 branch, respectively) which are less pronounced in the underdoped state, because the partial "correlation gap" introduced by both, the incompressible Cu3d orbitals and the missing of the compressible Cu4s orbitals leads according to Eq. (18) to reduced insulatorlike CF's at the Cu ion. Compared with the insulating state, however, the anomalies are increased in the underdoped phase in particular for the Δ_1 branch. A more detailed discussion of the phonon anomalies is given below. Another difference of the theoretical results as compared with those of the insulating state given in Ref. 3 is of qualitative nature and is related to the axial polarized Λ_1 branches. In the modeling of the underdoped state we have partially incompressible regions, however, the total compressibility is never zero in this state, because a real space organization of the low lying charge excitations is allowed and a metallic (gapless) charge transport is enabled via the hole-doped O2p orbitals at the oxygen network in the CuO plane. As a consequence the A_{2u} mode splittings are closed due to metallic screening, in particular the very large "ferroelectric" mode splitting, observed and calculated in the insulating state[3,4] and the Λ_1 branch with the steep dispersion characteristic for metallic behavior, being absent in the insulating state, reappears as is visible from Fig. 2. Altogether, we conclude that our modeling of the insulating, underdoped, and optimally doped state of LaCuO is consistent with the measured phonon dispersion.

B. Qualitative discussion of the modeling of the electronic state in the cuprates

We now discuss some qualitative aspects of our modeling of the electronic state of the cuprates suggested by the phonon calculations. In the model for the underdoped state a metallic mobility behavior is mediated via the O2p component of the wave function localized at the oxygen network of the CuO plane where the holes are injected too, but blocked along the Cu-O links because of the large on-site repulsion of the Cu3d component. Thus, by this partial ordering we have hole rich and hole poor regions of the conducting carriers on a microscopic scale in a translational invariant way ultimately driven by competing energy contributions. Note, that the various inhomogeneous self-organized charge and spin ordered configurations discussed in the literature[23–25] formally can be considered as certain "defect structures" (e.g., stripes) of our model if the spin degrees of freedom are explicitly considered. In case such structures are experimentally observed they express the tendency to restore an insulating Mott state in certain extended (incompressible) regions of the material.

From an energetic point of view the ground state should simultaneously minimize the zero point kinetic energy of the doped charge carriers and the exchange energy where both compete which each other. Because of the incompressible localized Cu3d states the holes are expelled from the antiferromagnetic regions by Coulomb correlation. Thus, an independent particle picture where an electron feels a time-averaged local density of the other electrons with a corresponding local potential (such as, e.g., in LDA) no longer holds. In this way the exchange energy is optimized (no spins need to be switched because of the restricted motion of the holes) while on the other hand, there is a gain in kinetic energy in the hole rich regions by delocalization of the electronic structure (hopping of the holes) via the compressible, metallic O2p component of the wave function. At the same time the exchange energy can be neglected in this region of configuration space if the delocalization effect is strong enough. Spin degrees of freedom and their correlations are not explicitly included in our modeling but implicitly support the latter because residual antiferromagnetic correlations can lead to an additional lowering of the kinetic energy by virtually hopping to the Cu3d states. This correlates the charge transport in the regions of excess charge to the remaining antiferromagnetic spin order in the hole poor regions at the Cu sublattice. So, we have a picture that can be regarded as resulting from a kind of separation of spin and

charge, being mutually relevant in different regions of the CuO plane. Low energy charge excitations occur in the hole rich regions where spin effects are depressed but are blocked in the hole poor regions, where the spin degrees of freedom are most important at low energy and high-energy (virtual) CF's induce an antiferromagnetic coupling on the Cu sublattice.

Then, in our modeling of the metallic state at higher doping the Cu3*d* and the additionally allowed delocalized Cu4*s* component become compressible, metallic. The incompressibility of Cu3*d* can be thought to be destroyed by an increased population of the Cu4*s* orbital. In Ref. 26 it has been shown that the Cu4*s* admixture to the electronic states of the HTSC is relevant and due to a gain in correlation energy. The dominant charge transfer resulting from the atomic correlations is from the localized Cu3*d* to the more delocalized Cu4*s* orbitals. The calculations in Ref. 26 are based on an *ab initio* method (local ansatz method) that adds correlations as corrections to a single-particle self-consistent ground state obtained from a Hartree-Fock calculation. An increased hybridization of Cu4*s* with the $pd\sigma$ orbitals can be expected to further relaxing the kinetic energy when doping is increased. As a consequence, the blocking of the metallic charge response at the Cu sites in the underdoped state is lifted and metallic behavior is now also possible via the CuO links. Altogether, this seems to be consistent with an emerging quasiparticle picture, a progressively weakening of the antiferromagnetic fluctuations and the development of a well defined Fermi surface as described by the sum rules from Eqs. (22) and (23) in our approach. The growing importance of the Cu4*s* component in the wave function leading to enhanced delocalized CF's at the Cu sites in the screening process is also mapped to a corresponding renormalization of the phonon anomalies as compared to the situation where the latter are neglected, see Ref. 27 and the discussion below. So, from our calculation additionally to Cu3*d* and O2*p* an increasing contribution of the delocalized Cu4*s* component to the metallic state of the cuprates is important to understand the charge response and the corresponding phonon softening in the real material at least at higher doping levels.

The importance of the Cu4*s* orbital for a realistic description of the electronic structure of the HTSC's has also been pointed out in Refs. 28 and 29. In the latter work, the hopping range has been identified as an essential material-dependent parameter and the intralayer hopping beyond nearest neighbors as well as the interlayer hopping proceeds via the Cu4*s* orbital. It is further concluded that materials with higher $T_{C,\max}$ have larger hopping ranges and in materials with highest $T_{C,\max}$ the axial orbital, essentially a hybrid between Cu4*s*, Cu3d_{3z^2-1}, and apical oxygen $2p_z$, is almost pure Cu4*s*. Moreover, the importance of Cu4*s* for an accurate description of the partial charge distributions in the HTSC's is pointed out applying the "local ansatz" *ab initio* method, which allows one to add correlations as corrections to a Hartree-Fock ground state[26] or density functional theory,[30] respectively.

Now we address the question concerning the possible nature of a superconducting state of the HTSC's that would be consistent with our modeling of the normal state. The suppression of the local CF's in our model for the underdoped state related to the incompressible Cu3*d* orbitals due to the large on-site repulsion competes with the superconductivity because of the enhanced phase fluctuations according to the number-phase uncertainty relationship $\Delta N \Delta \phi \geq 1$. In such a phase disordered superconductor pairing without long-range phase coherence is possible, i.e., there is an intermediate temperature range ($T > T_C$) where electron pairs exist which have not condensed. Such a precursor pair formation scenario is, for example, discussed in context with a kinetic energy driven pairing mechanism related to certain self-organized local charge inhomogenities in form of stripes[23,24] where pairing originates from strong repulsive interactions. Pair formation is thought to be realized in form of spin singlet pairs resulting in a spin gap by the "spin gap proximity" effect[25] because it seems favorable that, under appropriate circumstances, the pairs can spread out somewhat into the antiferromagnetic neighborhood of a stripe. However, up to now there is no experiment that proves the pairing is either kinetic energy driven or due to stripes. Note in this context, that the stripe scenario has been questioned by recent experiments which find that the observed nanoscale disorder in the HTSC's is due to dopant disorder.[31] Moreover, if the possibility of precursor pairs of some kind is theoretically explored, the strong nonlocal EPI found in our calculations expressed by the corresponding large changes of the self-consistent potential an electron feels according to Eq. (21), in particular for the generic phonon anomalies[32] and even larger for the nonadiabatic *c*-axis phonons,[1,4] should be taken into account in the electronic self-energy and the polarizability in addition to the short-ranged electron-electron repulsion that leads to spin and charge correlations in a many body treatment of a preformed pair state and the resulting gaps in the normal as well in the superconducting state. For a recent review of the important role of the EPI for the normal state properties and the pairing in the HTSC's we also refer to Ref. 33. Altogether, in the normal state one can expect two types of gaps in our modeling for the underdoped HTSC's the "correlation gap" and consistent with that modeling possibly a "precursor pairing gap" which are both linked by the short-ranged correlations introduced through the localized, incompressible Cu3*d* orbitals. While the former gap should correspond to the high-energy pseudogap seen in ARPES, the latter might be related to the low-energy gap found by the same experimental technique.[6]

Different from the underdoped state in our modeling of the optimally doped metallic state *all* the orbitals become compressible, metallic with enhanced CF's particularly in the Cu4*s* orbitals. So, we have a qualitative change to an electronic ground state with a well defined Fermi surface. In such a state a Fermi surface instability with a simultaneous evolution of pairs of quasiparticles would be consistent with the normal state and can lead to a BCS-type ordering. With regard to predominantly a phase ordering transition in the underdoped state optimal doping with a maximal T_C can be thought of as defining a gradual crossover to an overdoped state with predominantly a BCS-type pairing transition. Arguments in favor of such a crossover scenario also have been presented in Refs. 23 and 24.

According to the modeling of the charge response supported by our phonon calculations there are higher energy

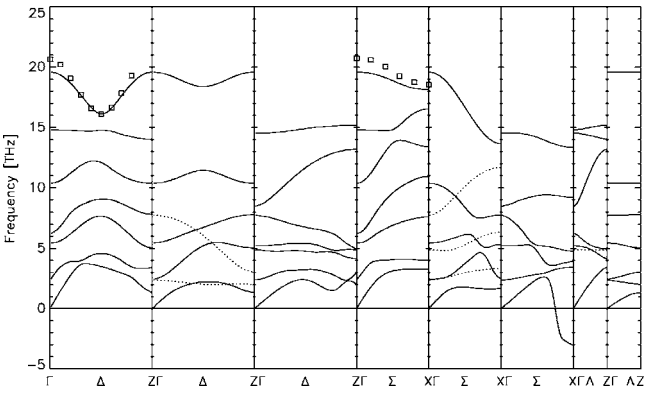

FIG. 3. Calculated phonon dispersion of LaCuO in the main symmetry directions as in Fig. 1 within the model for the overdoped state. The symbols indicate the experimental results for $La_{1.7}Sr_{0.3}CuO_4$ of the branches with the phonon anomalies (Ref. 19).

CF's related to the localized Cu3*d* orbital and low energy CF's of the more delocalized O2*p* and especially the Cu4*s* orbitals and a critical mixing of both via a population of Cu4*s* and a corresponding change of the populations of Cu3*d* and O2*p* and the related hybridization obviously is required to achieve $T_{C,\max}$ in the optimally doped material. The localization-delocalization transition in the normal state expressed as an incompressibility-compressibility transition of the Cu3*d* states corresponds to a phase ordering-pairing transition in the superconducting state.

C. Doping dependent anomalous phonon branches–Nonlocal dynamic charge inhomogenities

Next, we report calculations of the phonon dispersion for the overdoped state of LaCuO which can be compared with recent experimental results for the phonon anomalies.[19] An important message from these calculations is a further growing of the importance of the delocalized Cu4*s* component in the electronic wave function which seems consistent with an improved Fermi liquid quasiparticle picture, an increased coupling along the *c* axis and the dying out of the antiferromagnetic correlations, and an EPI which becomes more local.

In earlier calculations[1,27] we already have recognized the inclusion of Cu4*s* into the orbital basis as an important "tuning parameter" for the delocalization of the electronic structure of the HTSC's and the strength of the phonon anomalies. A growing occupation of the Cu4*s* orbital and a corresponding growth of the Cu(4*s*) element of the polarizability matrix leads to an increased softening of the anomalous phonon modes. So, enhancing Π(Cu4*s*) as compared with its value in the optimally doped state leading to the results shown in Fig. 1, gives very good agreement with the values measured for the anomalies in the overdoped state[19] and, moreover, provides a prediction for the complete phonon dispersion not measured so far, see Fig. 3.

In Fig. 4 we show a comparison of our calculated results for the anomalous phonon branches Δ_1 and Σ_1, in LaCuO with the corresponding experimental dispersion.[19] The strong doping dependence of the experimental phonon frequencies and thus of the EPI is clearly visible and very well accounted for by our modeling of the electronic state of the HTSC's discussed above. We have also included the phonon dispersion as obtained for the RIM representing approximatively the ionic local part of the charge response and the EPI in order to emphasize the large contribution due to the nonlocal EPI and screening in terms of the CF's. The displacement patterns of the phonon anomalies, i.e., the planar oxygen breathing mode at the *X* point O_B^X and the oxygen half-breathing mode $\Delta_1/2$ are displayed in Fig. 5. For symmetry reasons there are only CF's at the silent Cu ion allowed in O_B^X and not on the moving O_{xy} ions while in $\Delta_1/2$ in addition to the CF's at the Cu ion also CF's can be excited at the silent oxygens. This leads to an additional source of softening in case of $\Delta_1/2$ as compared to O_B^X and the larger renormalization of the frequencies found in our calculations and the experiments.[19,34] As already mentioned the enhanced softening in the overdoped doped state can be attributed to the growing Cu4*s* component in the electronic state and the related CF's at low energy. Moreover, the local character of the EPI is increased being dominant in a normal metal and superconductor, with delocalized electrons.

A word should be said concerning the importance of a correct representation of the on-site Coulomb repulsion U_d related to the localized Cu3*d* states and their effect on the nonlocal EPI by suppressing low energy CF's. The onsite parameters, such as U_d for the Cu3*d* orbitals, are defined in our modeling using Eq. (13) and taking the EDF κ, κ' to be localized at the same ion α in the crystal. An explicit expression for the calculation of these parameters is given by the following equations:[10]

$$U_{\kappa\kappa'} = \int dV \int dV' \frac{\rho_\kappa(\mathbf{r})\rho_{\kappa'}(\mathbf{r}')}{|\mathbf{r}-\mathbf{r}'|} + \int dV \rho_\kappa(\mathbf{r})\rho_{\kappa'}(\mathbf{r}) w[\rho_\alpha^0(\mathbf{r})] \tag{27}$$

with

$$w(\rho) = \frac{d\mu(\rho)}{d\rho}, \quad \mu(\rho) = \frac{d[\rho\epsilon(\rho)]}{d\rho}. \tag{28}$$

The relevant form factors ρ_κ, $\rho_{\kappa'}$ in Eq. (27) are defined by the $\rho_\lambda^{\mathrm{CF}}$ from Eq. (1) and ρ_α^0 is the unperturbed density of the ion α calculated in LDA-SIC as noted in Sec. II. The calculated value for U_d in units of e^2/a_B is 1.0050. The corresponding value for the more delocalized O2*p* and Cu4*s* states is 0.6708 and 0.3563, respectively. The large value for the Cu3*d* orbitals tends to suppress CF's at the Cu site according to Eqs. (15), (18), and (20), while the latter are strongly enhanced by the much smaller value for the Cu4*s* orbital. This again points to the important role of a Cu4*s* admixture in the electronic state and for the anomalous phonons in the cuprates.

A characteristic feature of the phonon anomalies is their selective sensitivity to U_d. A decrease of U_d enhances the CF's at the Cu ion considerably and leads in parallel to a softening of the phonon anomalies while the other phonon branches coupling to CF's are virtually not affected; see Fig. 6 for the $\Delta_1/2$ anomaly, where we have decreased U_d from

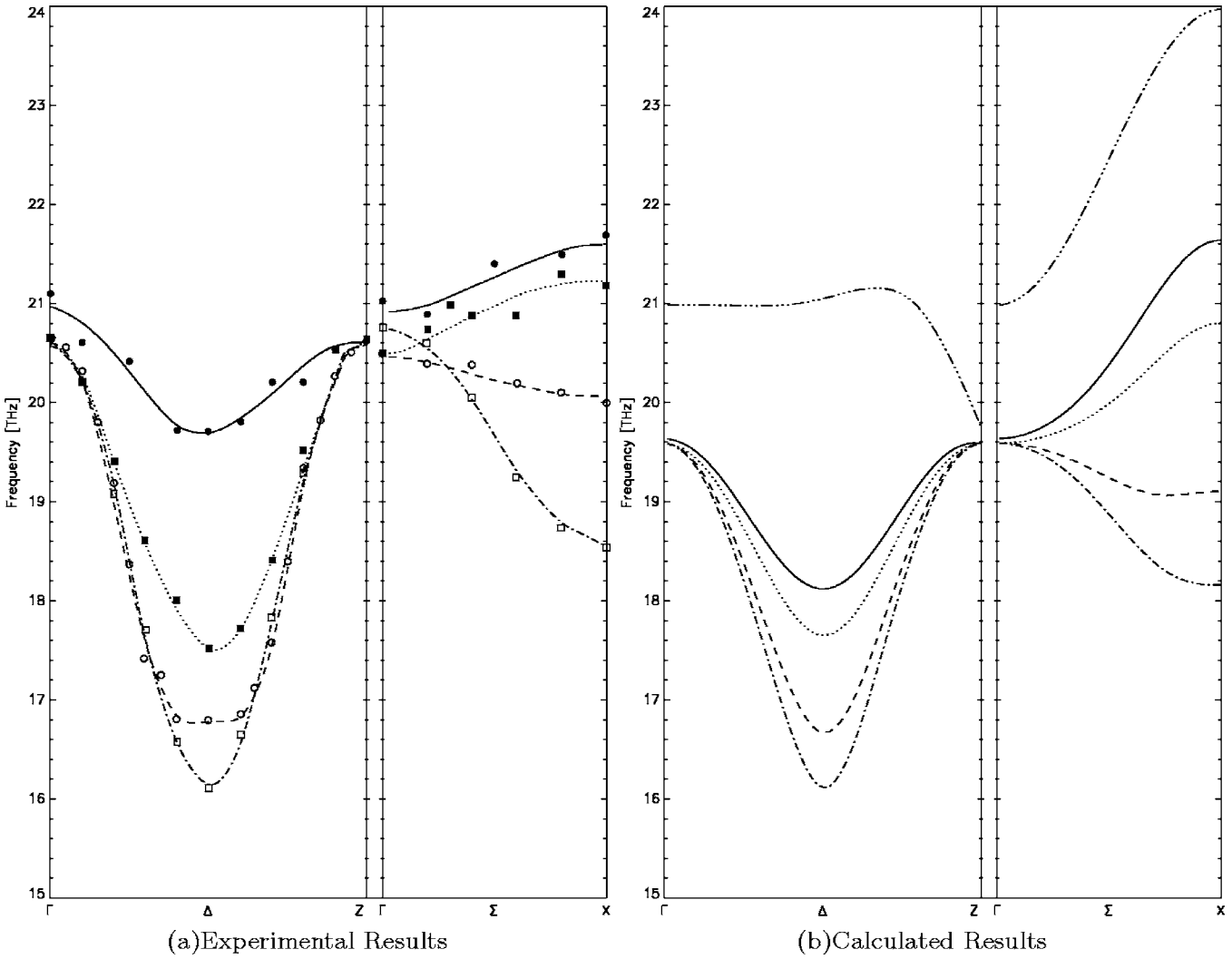

FIG. 4. (a) Experimental results for the highest Δ_1 and Σ_1 branch of $La_{2-x}Sr_xCuO_4$ for various doping levels (Ref. 19). •: $x=0.00$, ■: $x=0.10$, ∘: $x=0.15$, □: $x=0.30$. The lines are a guide to the eye. (b) Calculated results of the phonon branches shown in (a) as obtained within our model approach for the electronic state of the HTSC's. —: insulating state, ···: underdoped state, - - -: optimally doped state, –·– overdoped state. For comparison, the results for the *ab initio* RIM are shown (–···) in order to demonstrate the large influence of the nonlocal EPI effects in form of CF's on the dispersion.

its calculated value which by itself leads to the good quantitative agreement with the experiments in Fig. 2. A similar calculation for the Σ_1 branches even leads to an unstable planar breathing mode O_B^X being the highest mode in the insulating and underdoped state (other phonon branches coupling to CF's are only weakly modified). So, we conclude that our approximative calculation of U_d within DFT-LDA-SIC is sufficient to describe the correlation effect related to U_d on the phonon dynamics.

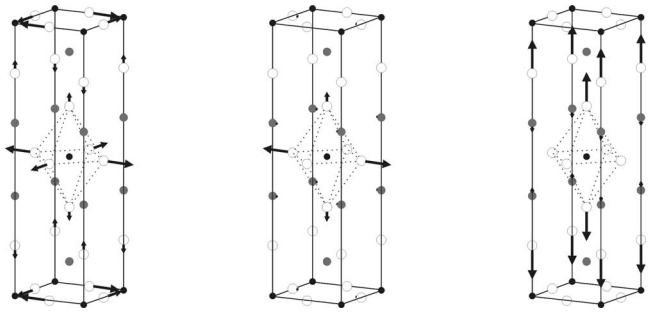

FIG. 5. Displacement patterns of the high-frequency oxygen bond-stretching modes of LaCuO. Left: planar breathing mode (O_B^X), middle: half-breathing mode ($\Delta_1/2$), right: apex-oxygen breathing mode (O_z^Z).

Local charge transfer from Cu3d into Cu4s orbitals due to atomic correlations has been shown in Ref. 26 to lead to a strong reduction (screening) of U_d for effective model Hamiltonian calculations. The influence on the phonon anomalies in LaCuO of such a screening effect for U_d already has been investigated in Ref. 5. In this work a model with a reduced set of EDF is used and CF's are only allowed for the Cu3d and the $O_{xy}2p$ states of the ions in the CuO plane. The contribution of more delocalized states, such as Cu4s or Cu4p, is simulated in this model by assuming a renormalizing (screening) of the on-site interaction U_d. Within such a procedure, the anomalous softening for $\Delta_1/2$ and O_B^X now seen in the experiments has been predicted and

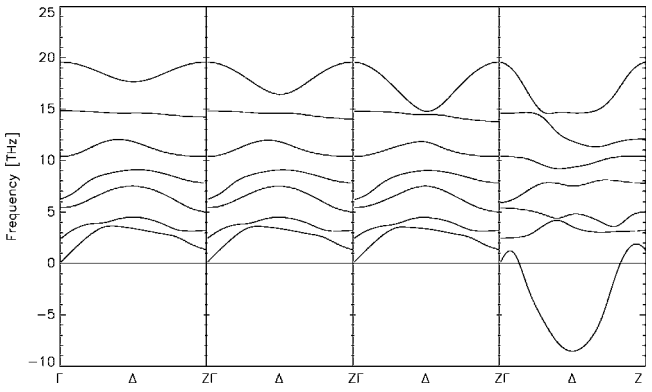

FIG. 6. Demonstration of the selective sensibility of the anomalous highest Δ_1 branch with respect to the on-site Coulomb repulsion U_d of the localized Cu3d orbitals. Only Δ_1 branches coupling to CF's are shown for the model of underdoped state of LaCuO. Using the calculated value for U_d (DFT-LDA-SIC, left panel) good agreement with the experimental data (Fig. 2) is obtained. In the remaining panels from left to right we arbitrarily have decreased U_d by the factor $\frac{2}{3}$, $\frac{1}{2}$, and $\frac{1}{3}$, respectively. For $\frac{1}{3}U_d$ the frequency of the $\Delta_1/2$ anomaly ($\approx$4.8 THz) is decreased towards an instability. In a corresponding calculation for the Σ_1 branches O_B^X even becomes unstable for $\frac{1}{3}U_d$.

related to the changes of the effective repulsive short-range Coulomb interaction at the Cu ion as an important physical parameter of the cuprates.

From an *ab initio* point of view the definite value for an effective U_d parameter which should be used in models with a reduced set of electronic degrees of freedom, such as the Hubbard models, which is widely used in the cuprates is by no means straightforward. Quite generally, a screening of the Coulomb interaction can be discussed within a renormalization scheme of the electronic density response as proposed in Refs. 11, 35, and 36, leading for the inverse dielectric matrix ε^{-1} to the following identity:

$$\varepsilon^{-1} = \varepsilon_r^{-1}\bar{\varepsilon}^{-1}, \tag{29}$$

with

$$\varepsilon_r^{-1} = (1+\bar{v}\Delta)^{-1}, \quad \bar{\varepsilon}^{-1} = (1+v\bar{\Pi})^{-1}, \quad \bar{v} = \bar{\varepsilon}^{-1}v. \tag{30}$$

This *general* factorization of the screening follows from an additive decomposition of the total polarizability Π into a suitable chosen renormalizing contribution ($\bar{\Pi}$) and a remaining part Δ that contains all the polarization processes not included in $\bar{\Pi}$, i.e.,

$$\Pi = \bar{\Pi} + \Delta. \tag{31}$$

Applying Eq. (29) to the bare Coulomb interaction v we obtain the screened interaction

$$V_{SC} = \varepsilon^{-1}v = (1+\bar{v}\Delta)^{-1}\bar{v}. \tag{32}$$

In Eq. (31) we can for example identify Δ with that part of Π which contains only 3d-3d transitions and $\bar{\Pi}$ with the remaining part of the total polarizability, i.e., by the other (renormalizing) electronic orbitals considered. Using this specific realization of the decomposition (31), we can extract from Eq. (32) that the interaction between the 3d electrons is provided by the interaction $\bar{v}$ defined by the screening processes of the other orbitals taking into account in Π.

In general the interaction between the 3d electrons $\bar{v}$ becomes frequency dependent (retarded) via the frequency dependence of the polarizability $\bar{\Pi}$, which could be calculated, e.g., at the RPA level, as in our treatment of the nonadiabatic regime. Summarizing, the interaction in a model reduced to the 3d degrees of freedom should be frequency dependent in contrast to the static U_d parameter assumed intuitively in Hubbard-like Hamiltonian approaches. From our considerations a static on-site interaction U_d should be identified with the partially renormalized interaction $\bar{v}$ in the low-energy limit, i.e., $U_d = \bar{v}(\omega \to 0)$. In this context we refer to recent work where it is found that a static value of U_d may not be the most appropriate one to use in effective model calculations.[37]

In summary, from our calculations we find that the phonon anomalies and the strong nonlocal EPI can be understood in terms of excited CF's in the outer shells of the ions, which are controlled by the kinetic contribution Π^{-1} to the electronic coupling coefficient C in Eq. (15) together with the contribution $\tilde{V}$, i.e., the Hartree- and exchange-correlation part of C. The interplay between strong correlation effects related to the localized Cu3d orbitals with their tendency to suppress CF's with low energy via $\tilde{V}$ and the contribution of the more extended orbitals O2p and Cu4s with a smaller (calculated) on-site repulsion which tends to enhance CF's is an essential feature for an understanding of the charge response and its influence on the phonons in a quantitative manner.

We have made explicit the charge response by calculating the phonon-induced charge density redistribution[1,2,27] for the phonon anomalies. According to these investigations the nonlocal EPI generates dynamic charge ordering via CF's in form of localized stripes of alternating sign in the CuO plane leading to an effective reduction of the energy visible in the anomalous softening. For the $\Delta_1/2$ mode the charge stripes point along the x or y axis, respectively, and for O_B^X along the diagonals in the CuO plane. These dynamical charge inhomogeneities would not be present in systems with local EPI, for example in a high density homogeneous electron gas prevailing in conventional metals. On the other hand, certain charge inhomogeneities observed in the HTSC's because of the reduced screening will couple nonlocally to the lattice and additional softening, compared with the system free of inhomogeneities, of the oxygen-bond-stretching-like modes (OBSM) can be expected due to the sensitivity of the latter to charge doping as seen in Fig. 4. For example, in the presence of a periodic charge order at a certain wave vector compatible with its period, anomalous softening and related mode splitting according to the broken rotational and translational symmetry should occur. Also nonperiodic, local charge inhomogeneities could lead to anomalous local OBSM via nonlocal EPI. These theoretical expectations are supported by recent experiments.[38] Here strong phonon softening of the OBSM has been observed in HTSC's at doping levels associated with static stripes at a wave vector corresponding to

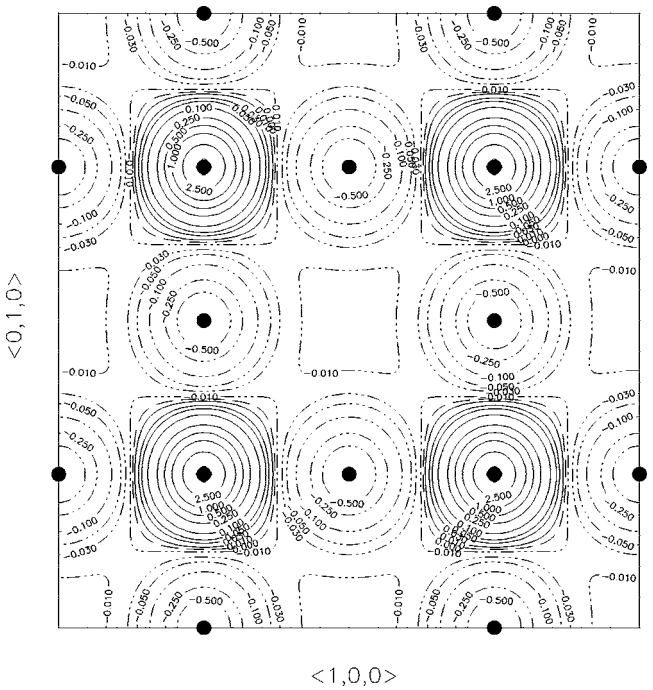

FIG. 7. Contour plot of the nonlocal part of the phonon-induced charge density redistribution for the O_z^Z mode (Fig. 5) in the model for the insulating state of LaCuO. The units are $10^{-4}e^2/a_B^3$. Full lines (—) mean that electrons are accumulated in the corresponding region of space and the lines (–···) represent regions where the electrons are pushed away, resulting in an intralayer charge transfer.

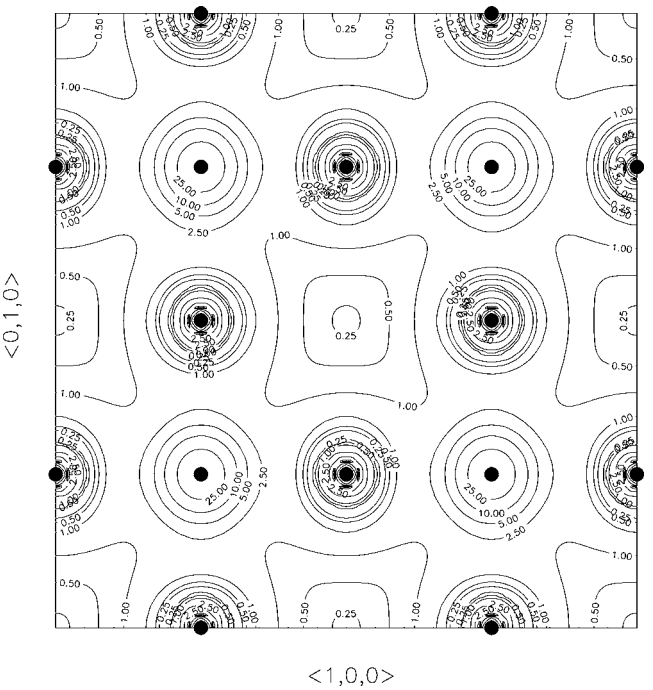

FIG. 8. Same as Fig. 7 but calculated with the model representing the optimally doped metallic state, resulting in CF's of the same sign in a CuO layer and a corresponding inter layer charge transfer.

the charge order. From the calculated results of the anomalies in Fig. 4 for the system with unbroken symmetry it can be expected that the strength of the anomalies in the inhomogeneous case sensitively should depend on the possibility of the inhomogeneous structure (e.g., stripes, static or dynamic with a sufficiently slow dynamics as compared to the time scale of the phonons) to be incompressible, insulating or compressible, metallic, respectively.

It is interesting to note that the electron correlation which result in an antiferromagnetic spin correlation in the HTSC's should favor the CF's in the OBSM and enhance screening against the tendency of a suppression of the CF's by the large on-site repulsion at the Cu, because if the spins in neighboring Cu orbitals were to be parallel, they would not both to be able to transfer to the neighboring oxygens or between the Cu ions themselves. On the other hand, if they are antiparallel they can do. Thus the phonon induced CF's depend implicitly on the spin degrees which may enhance the former and the EPI in an antiferromagnetic neighborhood as compared to a paramagnetic or a ferromagnetic one. Vice versa the nonlocal EPI of CF type is expected to generate antiferromagnetic spin fluctuations via the phonon-induced transferred charge between the Cu ions. This discussion around the phonon anomalies provides an example to illustrate, how coupled lattice-charge and spin degrees of freedom could act synergetically for pairing in the cuprates in a doping dependent way.

In addition $\Delta_1/2$ and O_B^X essentially polarized in the CuO plane another OBSM, i.e., the apex-oxygen (O_z) bond-stretching mode at the Z point (O_z^Z) polarized perpendicular to the CuO plane (Fig. 5) is of special interest for the cuprates due to the long-range Coulomb interaction in these compounds. Here we have the situation (similar as for the La_z^Z mode) that the displacement of the ions (O_z, La) in the ionic layers generates changes of the potential felt by the electrons in the CuO plane which themselves are responsible for the superconductivity. Such nonlocal coupling effects are an expression of the strong component of the ionic binding along the c axis in the HTSC's, i.e., these long-range Coulomb coupling effects are very special to this class of materials, and would not be possible in a convential metal or superconductor because of local-screening by a high-density electron gas. From the experiments in LaCuO (Refs. 19 and 34) we get the very remarkable result that O_z^Z is strongly renormalized when going from the insulating parent compound ($\approx$17 THz) to the optimally doped material ($\approx$11.5 THz). However, in the optimally doped probe a very large linewidth of about 4 THz appears that makes it difficult to localize the exact position of O_z^Z in the metallic phase. The massive line broadening has been interpreted within our nonadiabatic calculations[4] leading to a phonon-plasmon scenario for modes propagating in a very small region parallel to the c axis. From the calculations[1,4] we find a small region nearby the c axis with a nonadiabatic, insulatorlike charge response crossing over to a coherent adiabatic, metallic response outside this region. Moreover, an interconnection between the in-plane response and the size of the nonadiabatic inter-plane response is pointed out. So the electronic properties in the CuO plane take influence on the charge response perpendicular to the plane nearby the c axis.

The strong softening in the metallic state outside the small region of nonadiabatic charge response (for details see Refs.

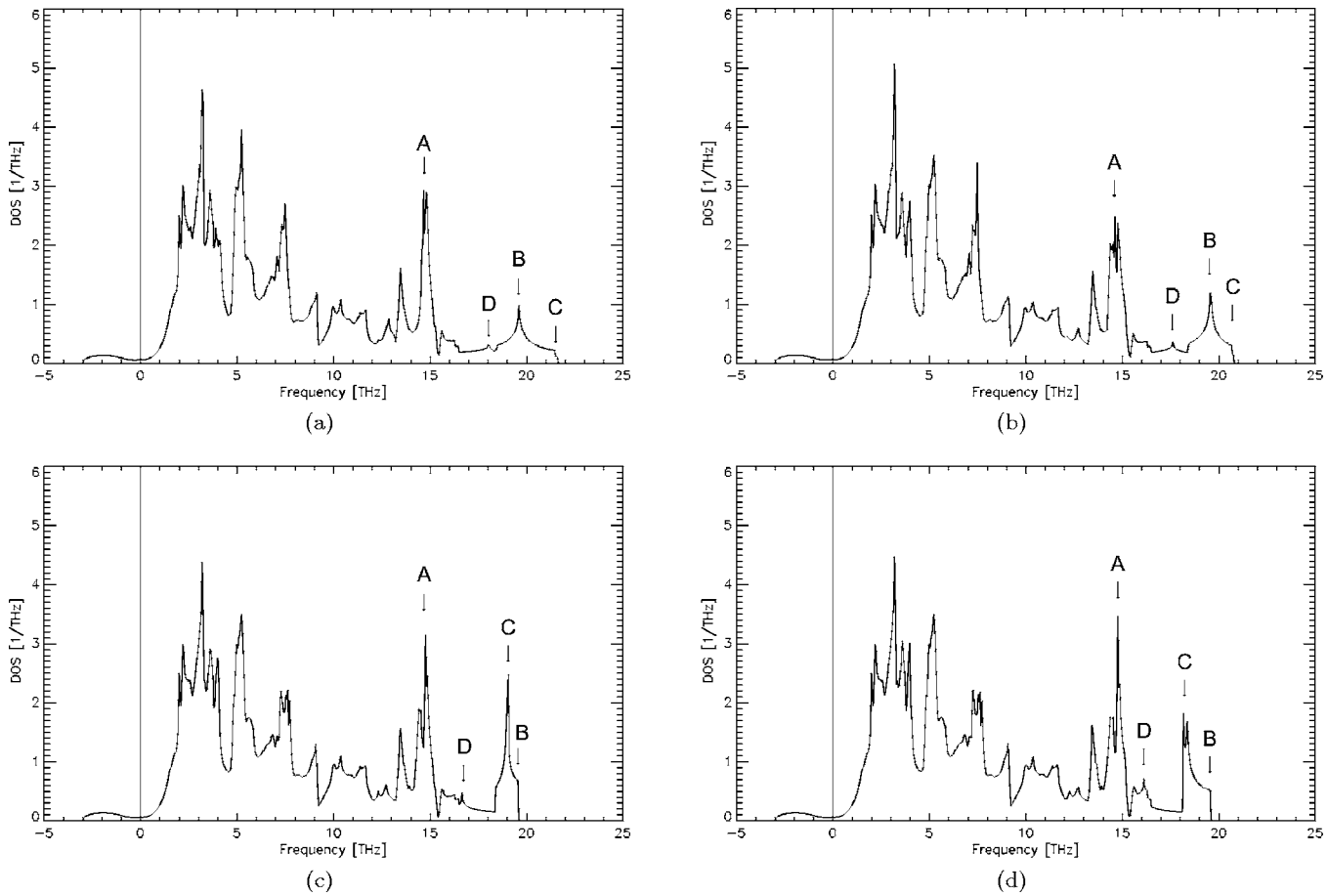

FIG. 9. Phonon density of states for LaCuO as calculated with the model for the insulating state (a), the underdoped state (b), the optimally doped state (c), and the overdoped state (d), respectively.

1 and 4) can physically be understood by comparing the phonon induced charge rearrangements for O_z^Z as calculated in the insulating and metallic state (Figs. 7 and 8), respectively. For the frequencies we find a renormalization of about 3 THz from 17.13 THz in the insulator to 14.17 THz in the metal, compare with the adiabatic phonon dispersion in Fig. 1 where O_z^Z is the second highest frequency of the Λ_1 branches at the Z point. A large EPI for the O_z^Z mode in the metallic state of LaCuO has also been calculated in Ref. 39 and attributed to a combination of weak screening along the c axis and nonlocal Madelung-like interactions. The importance of such long-ranged ionic contributions to coupling also has been pointed out in Refs. 40–43.

As can be extracted from Fig. 5 for O_z^Z the apex oxygens move in phase against the CuO layers. So, because of the weak screening one can expect this vibration to induce CF's in the CuO planes. These CF's, however, are qualitatively different in the insulating and the metallic state, respectively, because of the gap for charge excitations in the insulator. This helps to understand the anomalous softening of the mode during the insulator-metal transition. As has been shown in Ref. 5 the CF's $\delta\zeta_\kappa(\mathbf{q}\sigma)$ from Eq. (18) are constrained in the insulator with CF's allowed at the Cu and O_{xy} sublattices according to the following sum rule:

$$\sum_\kappa \delta\zeta_\kappa(\Lambda\sigma) = 0. \tag{33}$$

The sum over κ denotes the CF's in the CuO layer. $\Lambda \sim (0,0,1)$, so Eq. (33) particularly holds at the Z point of the Brillouin zone. In contrast to the constraint expressed by Eq. (33) for the insulating state, which means that local charge neutrality of the cell is maintained under a perturbation due to O_z^Z, no such a restriction is present for the metallic state. Unlike for LaCuO in the insulating state, where only intra layer charge rearrangements according to the sum rule Eq. (33) are allowed (Fig. 7), in the metallic state O_z^Z induces CF's at Cu and O_{xy} that have the same sign in the whole CuO layer (Fig. 8). This finally leads to CF's of alternating sign in consecutive CuO layers, i.e., to an inter plane charge transfer in the adiabatic regime that provides an effective screening mechanism for the long-range Coulomb interactions and generates the anomalous mode softening of O_z^Z during the insulator-metal transition.

D. Phonon density of states

In the last topic of this paper we present calculations for the phonon-density of states of LaCuO according to our modeling of the insulating, underdoped, optimally, and overdoped state of the HTSC's. Experimental studies by inelastic neutron spectroscopy of the phonon-density of states of LaCuO report unusual shifts for high-frequency OBSM during the insulator-metal transition indicating a strong EPI.[44]

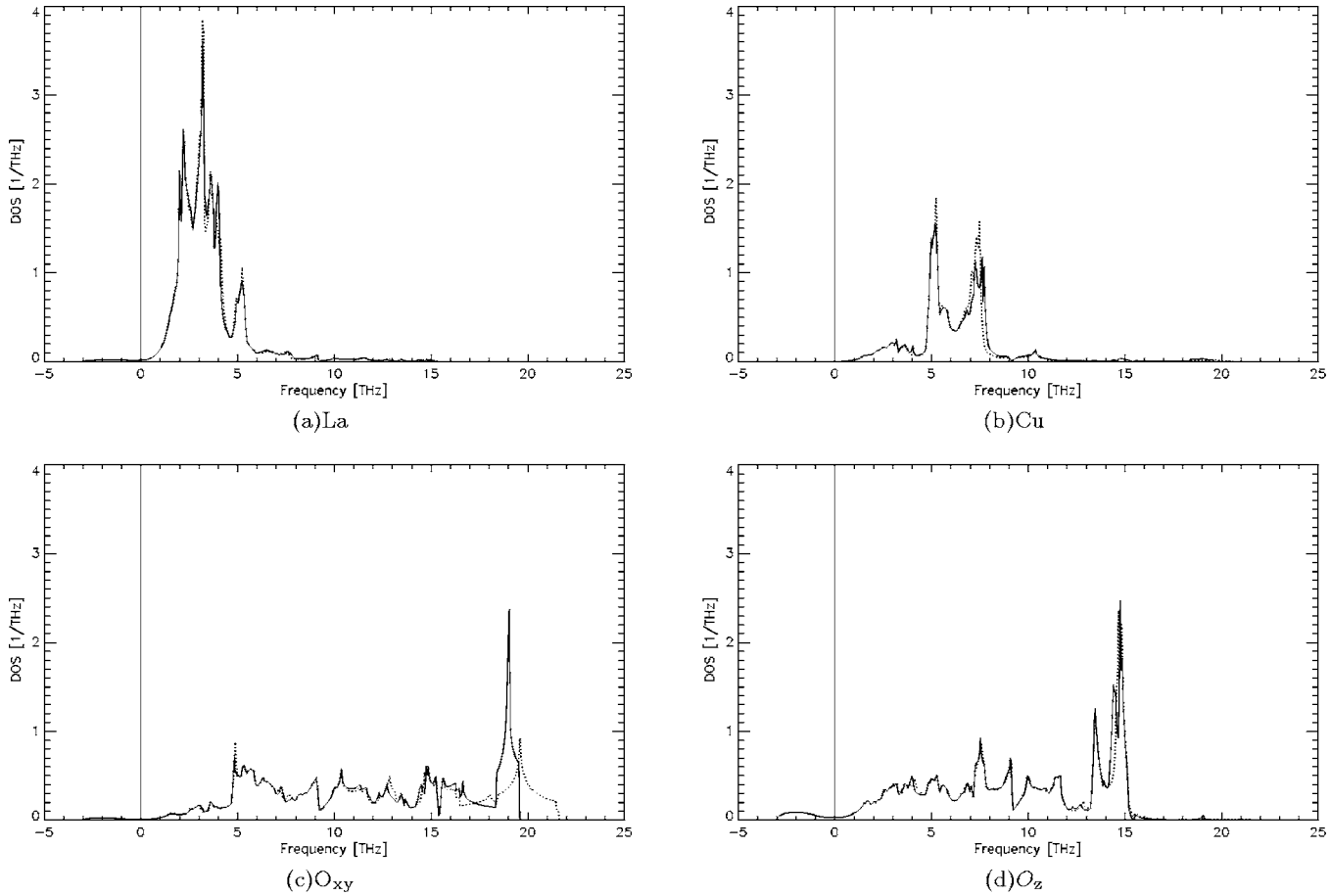

FIG. 10. Comparison of the atom resolved phonon density of states of LaCuO between the insulating state ⋯ and the optimally doped metallic state —.

Similar results are found for LaCuO in Ref. 45 where in addition to a shift of the high-frequency part of the spectrum to lower frequencies the development of "new" oxygen lattice vibrations centered in the optimally doped probe around 70 meV are observed near the doping induced insulator-metal transition and attributed to the mixing of these vibrations with metallic CF's.

Our calculations for the phonon density of states displayed in Figs. 9 and 10 allow for a detailed study of the changes of the spectrum during the insulator-metal transition. With the help of the calculated atom-resolved phonon-density of states in Fig. 10 and the phonon dispersion the characteristic modes indicated in Fig. 9 can be identified. The peak denoted as A is caused by vibrations of the apex oxygen O_z. B is related to the high-frequency oxygen vibrations E_u at the Γ point polarized in the CuO plane. C is the planar oxygen breathing mode O_B^X and D results from the oxygen half-breathing mode ($\Delta_1/2$ mode). In agreement with the experiments we find globally a shift of the high-frequency part of the phonon-density of states and also the development of spectral weight [peak D, see also Fig. 10(c)] passing from the insulating to the metallic state which we can assign to the $\Delta_1/2$ anomaly at 69 meV in our calculations for the optimally doped phase. Thus, the "new" oxygen lattice vibrations found in the experiments consist dominantly of the half-breathing modes, as supposed in Ref. 45. An important change of the spectrum related to the insulator-metal transition can be extracted from Figs. 9 and 10, because $B(E_u)$ and $C(O_B^X)$ are interchanged. So we have not just a global softening but also a very characteristic rearrangement of the high-frequency part of the spectrum, linked to the development of the phonon anomalies and the corresponding softening upon doping.

IV. SUMMARY

Within our microscopic modeling of the insulating, underdoped, optimally, and overdoped electronic state of the HTSC's we have performed calculations for LaCuO of the complete phonon dispersion curves, dynamic charge inhomogeneities induced by nonlocal EPI and the total- and atom-resolved phonon density of states. Our calculations emphasize the role of the doping dependence of the generic phonon anomalies and their selective sensitivity to both localization (correlation) effects provided by the Cu3d orbitals and delocalization effects via the Cu4s states. Thus, these anomalies are suitable probes to mirror the localization-delocalization transition of the electronic structure of the cuprates in terms of phonons. We have found good agreement with the corresponding measured phonon dispersion and phonon-density of states and have presented an interpretation of the results. In order to reach these results, both, long-

ranged Coulomb interactions of ionic origin as well as short-ranged repulsive interactions together with a sufficient set of orbital degrees of freedom are necessary. A purely ionic model leads to a considerable overestimation of the width of the phonon spectrum and to unstable branches in addition to the tilt mode. Including additionally covalent corrections a suitable starting model for the HTSC can be found that cures the disadvantages of the pure ionic description. Using such a model as an unprejudiced rigid reference system the effects of the important nonlocal nonrigid electronic polarization processes in terms of localized CF's and DF's have been studied. The latter localized screening effects and not a homogeneous electron gas screening allows for a quantitative calculation of the phonon anomalies and the dispersion. By the present investigations our earlier studies have been extended to the underdoped and overdoped state. Predictions of the dispersion in the latter case have been made.

An important aspect of the calculations, besides the efforts to explore the phonon dynamics and the EPI in the HTSC's as strongly correlated systems, where these topics presently are not well understood, in particular in the insulating and underdoped state, is to give additional support to our modeling of the electronic state. This is achieved in terms of consecutive orbital selective incompressibility-compressibility transitions. Such a modeling of the normal state qualitatively also provides a possible picture of the superconducting state that points from a phase ordering transition in the underdoped regime to a BCS-like pairing transition for higher doping. Optimal T_C should mark a gradual crossover point. The localization-delocalization crossover in our approach corresponding to a phase ordering-pair ordering crossover in the superconducting state is essentially related to the increase of an occupation with doping of the delocalized Cu4*s* orbitals progressively mixing into the Cu3*d*-O2*p* dominated electronic state of the underdoped material. Simultaneously an emerging quasiparticle picture with a well defined Fermi surface is consistent with our modeling upon doping. Finally, the strong and material specific nonlocal EPI effects found in the calculations demonstrate the important role of the phonons for the physics of the cuprates.

*Electronic address: falter@nwz.uni–muenster.de

[1] C. Falter, Phys. Status Solidi B **242**, 78 (2005).
[2] C. Falter and G. A. Hoffmann, Phys. Rev. B **61**, 14 537 (2000).
[3] C. Falter and F. Schnetgöke, Phys. Rev. B **65**, 054510 (2002).
[4] C. Falter, G. A. Hoffmann, and F. Schnetgöke, J. Phys.: Condens. Matter **14**, 3239 (2002).
[5] C. Falter, M. Klenner, and W. Ludwig, Phys. Rev. B **47**, 5390 (1993).
[6] A. Damascelli, Z. Hussain, and Z.-X. Shen, Rev. Mod. Phys. **75**, 473 (2003).
[7] T. Yoshida, X. J. Zhou, T. Sasagawa, W. L. Yang, P. V. Bogdanov, A. Lanzara, Z. Hussain, T. Mizokawa, A. Fujimori, H. Eisaki, Z.-X. Shen, T. Kakeshita, and S. Uchida, Phys. Rev. Lett. **91**, 027001 (2003).
[8] T. Timusk and B. Statt, Rep. Prog. Phys. **62**, 61 (1999).
[9] P. B. Allen, Phys. Rev. B **16**, 5139 (1977).
[10] C. Falter, M. Klenner, G. A. Hoffmann, and F. Schnetgöke, Phys. Rev. B **60**, 12 051 (1999).
[11] C. Falter, Phys. Rep. **164**, 1 (1988).
[12] C. Falter, M. Klenner, and G. A. Hoffmann, Phys. Rev. B **52**, 3702 (1995).
[13] J. P. Perdew and A. Zunger, Phys. Rev. B **23**, 5048 (1981).
[14] H. Krakauer, W. E. Pickett, and R. E. Cohen, J. Supercond. **1**, 111 (1998).
[15] S. Y. Savrasov and O. K. Andersen, Phys. Rev. Lett. **77**, 4430 (1996).
[16] C.-Z. Wang, R. Yu, and H. Krakauer, Phys. Rev. B **59**, 9278 (1999).
[17] K. P. Bohnen, R. Heid, and M. Krauss, Europhys. Lett. **64**, 104 (2003).
[18] S. L. Chaplot, W. Reichardt, L. Pintschovius, and N. Pyka, Phys. Rev. B **52**, 7230 (1995).
[19] L. Pintschovius, Phys. Status Solidi B **242**, 30 (2005).
[20] R. E. Cohen, W. E. Pickett, and H. Krakauer, Phys. Rev. Lett. **62**, 831 (1989).
[21] R. E. Cohen, W. E. Pickett, L. L. Boyer, and H. Krakauer, Phys. Rev. Lett. **60**, 817 (1988).
[22] M. J. De Weert, D. A. Papaconstantopoulos, and W. E. Pickett, Phys. Rev. B **39**, 4235 (1989).
[23] E. W. Carlson, V. J. Emery, S. A. Kivelson, and D. Orgad, in *The Physics of Conventional and Unconventional Superconductors*, edited by K. H. Bennemann and J. B. Ketterson (Springer-Verlag, Berlin, 2004).
[24] S. A. Kivelson and E. Fradkin, cond-mat/0507459 (unpublished).
[25] V. J. Emery, S. A. Kivelson, and O. Zachar, Phys. Rev. B **56**, 6120 (1997).
[26] G. Stollhoff, Phys. Rev. B **58**, 9826 (1998).
[27] C. Falter, M. Klenner, G. A. Hoffmann, and Q. Chen, Phys. Rev. B **55**, 3308 (1997).
[28] O. K. Andersen, A. I. Liechtenstein, O. J. Jepsen, and F. Paulsen, J. Phys. Chem. Solids **56**, 1573 (1995).
[29] E. Pavarini, I. Dasgupta, T. Saha-Dasgupta, O. Jepsen, and O. K. Andersen, Phys. Rev. Lett. **87**, 047003 (2001).
[30] E. P. Stoll, P. F. Meier, and T. A. Claxton, J. Phys.: Condens. Matter **15**, 7881 (2003).
[31] K. McElroy, Jinho Lee, J. A. Slezak, D.-H. Lee, H. Eisaki, S. Uchida, and J. C. Davis, Science **309**, 1048 (2005).
[32] C. Falter and G. A. Hoffmann, Phys. Rev. B **64**, 054516 (2001).
[33] M. L. Kulić and O. V. Dolgov, Phys. Status Solidi B **242**, 151 (2005).
[34] L. Pintschovius and W. Reinhardt, in *Neutron Scattering in Layered Copper-Oxide Superconductors*, edited by A. Furrer, Vol. 20 of Physics and Chemistry of Materials with Low Dimensional Structures, (Kluwer Academic, Dordrecht, 1998).
[35] C. Falter and M. Selmke, Phys. Rev. B **21**, 2078 (1980).
[36] C. Falter and M. Selmke, Phys. Rev. B **24**, 586 (1981).
[37] F. Aryasetiawan, K. Karlsson, O. Jepsen, and U. Schönberger, cond-mat/0603138 (unpublished).
[38] D. Reznik, L. Pintschovius, M. Ito, S. Iikubo, M. Sato, H. Goka, M. Fujita, K. Yamada, G. D. Gu, and J. M. Tranquada, cond-mat/0512063 (unpublished).
[39] H. Krakauer, W. E. Pickett, and R. E. Cohen, Phys. Rev. B **47**,

1002 (1993).
[40] T. Jarlborg, Solid State Commun. **67**, 297 (1988); **71**, 669 (1989).
[41] R. Zeyher, Z. Phys. B: Condens. Matter **80**, 187 (1990).
[42] V. L. Ginzburg and E. G. Maksimov, Physica C **235-240**, 193 (1994).
[43] E. G. Maksimov, Phys. Usp. **43**, 965 (2000).
[44] R. Renker, F. Gompf, P. Adelmann, Th. Wolf, H. Mutka, and A. Dianoux, Physica B **180/181**, 450 (1992).
[45] R. J. McQueeney, J. L. Sarrao, P. G. Pagliuso, P. W. Stephens, and R. Osborn, Phys. Rev. Lett. **87**, 077001 (2001).